Bacterial Expression, Characterization, and Disulfide Bond Determination of Soluble Human NTPDase6 (CD39L2) Nucleotidase: Implications for Structure and Function†

Vasily V. Ivanenkov, Deirdre M. Murphy-Piedmonte, and Terence L. Kirley*

Department of Pharmacology and Cell Biophysics, College of Medicine, University of Cincinnati, P.O. Box 670575, Cincinnati, Ohio 45267-0575

Received July 1, 2003; Revised Manuscript Received August 13, 2003

ABSTRACT: The ectonucleoside triphosphate diphosphohydrolases (NTPDases) control extracellular nucleotide concentrations, thereby modulating many important biological responses, including blood clotting and pain perception. NTPDases1−4 are oligomeric integral membrane proteins, whereas NTPDase5 (CD39L4) and NTPDase6 (CD39L2) are soluble monomeric enzymes, making them more amenable to thorough structural and functional analyses than the membrane-bound forms. Therefore, we report here the bacterial expression, refolding, purification, and biochemical characterization of the soluble portion of human NTPDase6. Consistent with the enzyme expressed in mammalian cells, this recombinant NTPDase6 efficiently hydrolyzes GDP, IDP, and UDP (specific activity of approximately 50000 μmol mg^{-1} h^{-1}), with slower hydrolysis of CDP, ITP, GTP, CTP, ADP, and UTP and virtually no hydrolysis of ATP. The K_m for GDP (130 ± 30 μM) is similar to that determined for the soluble rat NTPDase6 expressed in mammalian cells. The secondary structure of the refolded enzyme was determined by circular dichroism to be 33% α-helix, 18% β-sheet, and 49% random coil, consistent with the secondary structure predicted from the amino acid sequence of soluble NTPDase6. Four of the five cysteine residues in the soluble NTPDase6 are highly conserved among all the NTPDases, while the fifth residue is not. Mutation of this nonconserved cysteine resulted in an enzyme very similar to wild type in its enzymology and secondary structure, indicating that this cysteine exists as a free sulfhydryl and is not essential for structure or function. The disulfide pairing of the other four cysteine residues was determined as Cys^{249}−Cys^{280} and Cys^{340}−Cys^{354} by HPLC and mass spectral analysis of tryptic peptides. Due to conservation of these cysteine residues, these two disulfide bonds are likely to exist in all NTPDases. A structural model for NTPDase6, incorporating these and other findings obtained with other NTPDases, is proposed.

The ecto*n*ucleoside *trip*hosphate *d*iphosphohydrol*ases* (NTPDases)[1] are a family of enzymes that hydrolyze extracellular nucleoside di- and triphosphates and require divalent cations (e.g., Ca^{2+} or Mg^{2+}) for activity. There are six members of the NTPDase family characterized to date: four membrane-bound enzymes (NTPDase1−4) whose carboxy- and amino-terminal ends are anchored in the cell membrane and two soluble, excreted enzymes (NTPDase5 and NTPDase6) with cleavable N-terminal signal sequences (*1*). The NTPDases share seven highly conserved regions of homology (*2*−*5*), termed *a*pyrase *c*onserved *r*egions (ACRs), which are essential for catalytic activity.

By regulating the availability of extracellular nucleotides for use by ectokinases and purinergic receptors, human ectonucleotidases serve important physiological functions and have been implicated in many processes involving purinergic receptor systems, such as the modulation of platelet aggregation (*6*), smooth muscle contraction (*7*), and pain perception (*8*, *9*). Recent studies have shown that endothelial cell membrane CD39 (NTPDase1) (*6*, *10*, *11*) and a soluble version of CD39 (*12*, *13*) are potential therapeutic proteins that can control the ill effects of stroke and other ischemic pathologies by hydrolysis of ADP that regulates platelet activation and blood clotting. Other studies have demonstrated the release of soluble nucleotidases along with nucleotide (ATP) used as an agonist for neurotransmission and speculated as to the physiological importance of the release of such soluble nucleotidases for neurotransmitter inactivation (*14*−*16*).

The soluble human nucleotidase NTPDase6 (CD39L2) was discovered in 1998 (*17*), and its characterization has only been reported in a few studies, all utilizing mammalian cell

† This work was supported by NIH Grants HL59915 and HL72382 (both to T.L.K.).

* To whom correspondence should be addressed. Phone: 513-558-2353. Fax: 513-558-1169. E-mail: terry.kirley@uc.edu.

[1] Abbreviations: NTPDases, *n*ucleoside *trip*hosphate *d*iphosphohydrol*ases*; NTPDase6, nucleoside triphosphate diphosphohydrolase type 6; ACRs, apyrase conserved regions; B-PER, bacterial protein extraction reagent; CD, circular dichroism; HPLC, high-performance liquid chromatography; MALDI-TOF MS, matrix-assisted laser desorption ionization time-of-flight mass spectrometry; TCEP, tris(2-carboxyethyl)phosphine hydrochloride; TBP, tributylphosphine; ABD-F, 4-(aminosulfonyl)-7-fluoro-2,1,3-benzoxadiazole; MWCO, molecular weight cutoff; P_i, inorganic phosphate; *m*/*z*, mass-to-charge ratio; CHO, Chinese hamster ovary; TFA, trifluoroacetic acid; MOPS, 3-(*N*-morpholino)propanesulfonic acid; IPTG, isopropyl β-D-thiogalactopyranoside; DTT, dithiothreitol; IAA, iodoacetamide.

10.1021/bi035137r CCC: $25.00
Published on Web 09/16/2003

expressed enzymes (*18*−*20*). Thus, there is limited information concerning NTPDase6 enzymology, structure, and putative function(s). Braun et al. suggested that the membrane-bound form of rat NTPDase6 is associated with the Golgi apparatus and might support glycosylation reactions in the Golgi (*18*). Ford and co-workers reported that the gene encoding human NTPDase6 was expressed primarily in the heart (*20*) and suggested that the enzyme plays a functional role in the heart by modulating platelet aggregation via ADP hydrolysis.

NTPDase6 is a useful model system to study many aspects of the more complex, oligomeric, membrane-bound NTPDase ectonucleotidases. It has the advantage of being soluble and monomeric, making NTPDase6 more amenable to biochemical study and structural analyses than the membrane-bound forms. Here we demonstrate that bacterial expression and refolding are feasible for the soluble NTPDases, allowing purification of amounts of protein needed for future 3-D structural determination. NTPDase6 expressed in bacteria preferentially hydrolyzes GDP, IDP, and UDP, with slower hydrolysis of CDP, ITP, GTP, CTP, ADP, and UTP and virtually no hydrolysis of ATP. This substrate profile indicates that bacterially expressed NTPDase6 described in this work has biochemical properties similar to those of the mammalian cell expressed human NTPDase6 (*19*), as well as to those of rat brain NTPDase6, which is ~86% identical on the amino acid level with the human NTPDase6 (*18*).

Disulfide bonds are important for both proper folding and protein stability after folding. In addition, the determination of the disulfide architecture is very helpful for interpreting crystallography or NMR data used to elucidate the three-dimensional structures of proteins. Therefore, the disulfide bond architecture of NTPDase6 was determined in this study, resulting in identification of disulfides between Cys^{249}−Cys^{280} and Cys^{340}−Cys^{354}. These four cysteines are conserved in all NTPDases in regions of the proteins that should be noncytoplasmic. Therefore, it is likely that these two disulfide bonds exist as part of the disulfide architecture in all NTPDases. Cys^{139} exists as a free sulfhydryl in NTPDase6 and was replaced by serine via site-directed mutagenesis without affecting its nucleotidase activity, suggesting that this residue is neither functionally nor structurally essential. However, either oxidation or alkylation of this residue resulted in a decrease in enzyme activity, suggesting either a steric or an allosteric effect. On the basis of characterization of the disulfide architecture of NTPDase6, circular dichroism (CD) data, and regions of conservation among all the NTPDases, a secondary structural model of NTPDase6 is proposed. Thus, the bacterial expression, refolding, disulfide bond architecture, and secondary structure model reported in this work should facilitate the determination of the 3-D structure of this soluble NTPDase. In addition, the results presented in this study may facilitate the development of therapeutic proteins (e.g., anticoagulants) based on facile modification of the nucleotidase specificity of bacterially expressed NTPDase6 by experimental (site-directed mutagenesis) methods, as well as by computational (computer modeling) methods based on the yet to be determined 3-D structure.

MATERIALS AND METHODS

Materials. Plasmid purification kits and Ni-NTA−agarose were purchased from Qiagen Inc. The QuikChange site-directed mutagenesis kit and *Escherichia coli* XL-1 Blue competent cells were purchased from Stratagene. T4 DNA ligase was obtained from Invitrogen. The bacterial expression vector pET28a and the expression host *E. coli* BL21(DE3) cells were purchased from Novagen. The DNA Core Facility at the University of Cincinnati produced the synthetic oligonucleotides and performed DNA sequencing. *Nhe*I and S*al*I restriction endonucleases, glycerol, and dialysis tubing were from Fisher. B-PER, TCEP, and enhanced chemiluminescent reagents were purchased from Pierce. The anion-exchange QMA cartridge, 4−15% and 7.5% Tris−glycine gels were from Bio-Rad. ABD-F was purchased from Molecular Probes and from Dojindo Laboratories. Kanamycin, nucleotides, IPTG, glucose, thrombin, DTT, TBP, oxidized glutathione, reduced glutathione, and other reagents were from Sigma. The 30000 MWCO concentrators were from Amicon. Sequencing grade trypsin was from Roche Diagnostics. The 15 cm, 300 Å pore size, 4.6 mm C_{18} reverse phase column used to separate peptides was from Vydac. HPLC was performed using a Shimadzu CLASS-VP apparatus in the laboratory of Dr. John Maggio, University of Cincinnati. Relative fluorescence of treated HPLC fractions was assayed using a SPF-500C SLM Instruments spectrofluorometer. Mass spectral analysis was performed by the Department of Chemistry Mass Spectrometry Facility at the University of Cincinnati.

NTPDase6 Cloning and Sequencing. A Life Technologies human brain SuperScript cDNA library was screened for NTPDase6 (CD39L2) cDNA by enrichment of specific cDNA using the GeneTrapper cDNA positive selection system obtained from Gibco BRL, as described previously for the chicken NTPDase2 (*21*). The probe sequence used for the GeneTrapper selection encodes part of the human NTPDase6 protein near the N-terminus: GCC TAC ATC AAG TGG CAC CG (encoding AYIKWHR). The human brain NTPDase6 (CD39L2) clone isolated was termed "HB4", and its sequence has been deposited in GenBank (accession AY327581). Compared to the CD39L2 cDNA sequence reported by Chadwick and Frischauf (*17*), this clone has one "nonsilent" mutation in the soluble portion of the molecule, having a **C**TG sequence rather than **G**TG (Leu, not Val), encoding the sequence HETFKA**L**KPGLSA. At this site of apparent discrepancy (underlined and in bold type), the clone used in this work agrees with the NTPDase6 DNA sequence reported in the human genome project (as revealed by a BLAST search ref|NT_011387.8|Hs20_11544 Homo sapiens chromosome 20 genomic, base 25130520 is "C").

Protein Assay. Protein concentrations were determined using the Bio-Rad Coomassie Brilliant Blue G-250 dye binding technique according to the modifications of Stoscheck (*22*) using bovine serum albumin as a standard.

Polyclonal Antibody Production. The production of the polyclonal antiserum to the carboxy-terminal amino acid sequence of NTPDase6 and the affinity purification of antibodies from the antiserum have been described (*19*).

Electrophoresis and Western Blot Analysis. SDS−PAGE was performed following the method of Laemmli (*23*), using

4−15% precast gradient gels. The NTPDase6 samples were boiled for 5 min in SDS sample buffer containing 30 mM dithiothreitol prior to SDS−PAGE. Western blotting was performed as previously described using an antibody raised against a C-terminal NTPDase6 peptide (*19*).

Nucleotidase Assay. Nucleotidase activity was determined by measuring the amount of inorganic phosphate released from nucleotide substrates at 37 °C using a modification of the technique of Fiske and Subbarow (*24*) as previously described (*25*). Nucleotide hydrolyzing units are expressed in micromoles of P_i liberated per milligram of protein per hour, at a final nucleotide concentration of 2.5 mM, in the presence of 5 mM $CaCl_2$ or 5 mM $MgCl_2$.

Assays for determining K_m were performed using the more sensitive malachite green reagent (*26*). Nucleotidase activity was assayed by measuring inorganic phosphate released after 15 min incubation of NTPDase6 with GDP substrate, using a range of GDP concentrations from 0.0018 to 0.469 mM. Care was taken to ensure that less than 10% of the total GDP substrate at each concentration was consumed in all reactions. K_m and V_{max} values were determined by fitting data to a standard hyperbolic function, according to Michaelis−Menten kinetics, using the Origin 7 computer program. Means and errors for K_m and V_{max} values were obtained from multiple, independent experiments and fits.

Mutagenesis of NTPDase6 for Cloning into a Bacterial Expression Vector. To allow cloning of the NTPDase6 sequence into the bacterial expression vector pET28a, restriction endonuclease sites were introduced flanking the coding region. An *Nhe*I endonuclease site was introduced by site-directed mutagenesis 5′ to the cDNA sequence, and a *Sal*I restriction site was introduced at the 3′ end of the cDNA sequence encoding soluble NTPDase6. The NTPDase6 insert was ligated into pET28a bacterial expression vector (cut with the same endonucleases). Transformation into a nonexpression host (*E. coli* XL-1 Blue cells) allowed construct verification by DNA sequencing.

Expression of NTPDase6 in BL21(DE3) Cells. For bacterial expression, the NTPDase6 insert in the pET28a vector was transformed into *E. coli* BL21(DE3) cells. Five milliliters of LB broth containing 1% glucose and 60 μg/mL kanamycin was inoculated with 10 μL of frozen bacterial stock derived from a single colony of transformed BL21(DE3) cells and allowed to grow at 37 °C for 5 h. This 5 mL culture was added to 500 mL of LB broth (containing 1% glucose and 30 μg/mL kanamycin) and grown to an OD_{600} of approximately 0.5 before induction with IPTG (1 mM final concentration). After induction, the culture was grown for an additional 4 h at 37 °C, reaching an OD_{600} of approximately 1. Bacterial inclusion bodies were prepared using the Pierce B-PER reagent as previously described (*27*), typically yielding 40−50 mg of inclusion body proteins.

Preparative Refolding of NTPDase6 from Inclusion Bodies. Approximately 5 mg of NTPDase6 inclusion body preparation was solubilized in 5 mL of 6 M guanidine hydrochloride, 2 mM EDTA, and 5 mM DTT in 100 mM Tris-HCl, denatured by heating for 10 min at 60 °C, and then cooled to room temperature. Refolding was performed by dilution of the 5 mL sample into 250 mL of ice-cold buffer containing 100 mM Tris-HCl, 10 mM KCl, 250 mM NaCl, 2 mM $CaCl_2$, 2 mM $MgCl_2$, 500 mM (800 mM in some experiments) L-arginine hydrochloride, 2 mM reduced glutathione (GSH), and 0.4 mM oxidized glutathione (GSSG), pH 8.35, and proceeded for 2−3 days. Refolding experiments were performed at several different temperatures (ranging from 4 to 23 °C) to determine the optimum temperature for refolding. After refolding, the 255 mL NTPDase6 sample was dialyzed against three 4 L changes of 50 mM Tris-HCl, 250 mM NaCl, and 2 mM $CaCl_2$ (pH 8.0) for 2−3 days at 4 °C to decrease the high arginine concentration that interferes with the hexahistidine tag binding to Ni-NTA beads.

Purification of Refolded NTPDase6. The pET28a vector encodes a hexahistidine tag, N-terminal to the NTPDase6 insert, which allows purification of the protein on an immobilized metal affinity (Ni-NTA) column. Approximately 6 mL of Ni-NTA−agarose bead suspension (corresponding to a settled bead volume of approximately 3 mL) was washed three times with 10 mL of wash buffer containing 50 mM Tris-HCl, 250 mM NaCl, and 2 mM $CaCl_2$, pH 8.0. Approximately 300 mL of refolded and dialyzed NTPDase6 was added to the Ni-NTA−agarose beads, and the slurry was incubated on ice for at least 1 h with gentle, occasional mixing. The NTPDase6/Ni-NTA−agarose slurry was poured into a column, and the unbound fraction was collected. The column was washed seven times with 4 mL of wash buffer. NTPDase6 was eluted from the Ni-NTA column in four 2.5 mL fractions of wash buffer containing 200 mM imidazole, pH 8.0. Eluted NTPDase6 was immediately diluted into 10 mL of ice-cold wash buffer (to a final sample volume of 20 mL) to decrease the imidazole concentration and promote protein solubility. All fractions, including the unbound material, were assayed for GDPase activity in the presence of Ca^{2+}.

Thrombin Cleavage and Subsequent Anion-Exchange Chromatography of NTPDase6. Approximately 3 units of thrombin was added to 20 mL of partially purified NTPDase6, mixed thoroughly, and dialyzed overnight at 4 °C against 2 L of 50 mM Tris-HCl, 150 mM NaCl, and 2 mM $CaCl_2$, pH 8.0. This sample was further dialyzed versus 2 L of 20 mM Tris-HCl and 50 mM NaCl, pH 8.0. The dialyzed sample was centrifuged at 18000 rpm for 30 min at 4 °C. The supernatant was loaded onto a 1 mL strong anion-exchange (Bio-Rad QMA) cartridge equilibrated with approximately 40 mL of 20 mM Tris-HCl and 50 mM NaCl, pH 8.0, and the flow-through fraction was collected. The cartridge was washed twice with 2 mL of the equilibration buffer, and the wash fraction was combined with the flow-through fraction. This 24 mL NTPDase6 sample was concentrated to a volume of approximately 0.8 mL in a Centricon CentriPrep concentrator with a 30000 MWCO.

Mutation of the Nonconserved Cysteine Residue in Wild-Type NTPDase6. The sole nonconserved Cys^{139} residue in NTPDase6 was changed to serine via site-directed mutagenesis using the following sense primer: 5′ GGGGATGAC-**TCT**GTTTCCATCATGAACGG 3′. The codon responsible for the mutation is indicated in bold face. The antisense primer also required for mutagenesis is not shown. The presence of the desired C139S mutation was confirmed by DNA sequencing.

Tryptic Digestion and HPLC of NTPDase6 for Disulfide Determination. These experiments were performed on the C139S mutant of NTPDase6, which was shown (see below) to be very similar in enzymatic properties and secondary

structure to wild type. The lack of an unpaired cysteine residue in C139S would decrease the possibility for unwanted disulfide interchange occurring during proteolysis. Thus, 150 μg of refolded, active C139S NTPDase6 was dialyzed at 4 °C against buffer (100 mM MOPS−KOH, 4 mM $CaCl_2$, pH 7.0) and then clarified by centrifugation for 2 min at maximum speed in a microcentrifuge. Urea (115 mg) was added to and dissolved in 167 μL of the clarified sample, resulting in a final volume of approximately 240 μL and a urea concentration of approximately 8 M. The sample was incubated at room temperature for 20 min, and then 313 μL of buffer (100 mM MOPS−KOH, 4 mM $CaCl_2$, pH 7.0) and 407 μL of water were added, resulting in a final volume of approximately 960 μL containing 2 M urea, 50 mM MOPS−KOH, and 2 mM $CaCl_2$, pH 7.0. To this sample was added 30 μL of trypsin (0.5 μg/μL in 1 mM HCl) to give a final ratio of trypsin to NTPDase6 protein of approximately 1:10 (w/w). The trypsinolysis was allowed to proceed at 37 °C for 18 h. To this digest was added 10 μL of 10% TFA, and the sample was centrifuged for 2 min at maximum speed in a microcentrifuge. The supernatant was collected and injected onto a C_{18} HPLC column (Vydac) equilibrated in 0.1% TFA in water. Peptides were eluted with a gradient of acetonitrile in water (see figure legends for details of the gradients used), and both solvents contained 0.1% TFA. Fractions of 0.7 mL (1 min) were collected.

Fluorescence Assay for Peptides Containing Disulfides. NTPDase6 tryptic peptides separated by HPLC were analyzed for the presence of disulfides by reduction with TBP and labeling with a fluorescent reagent, ABD-F, as described (*28*). TBP was used as a reducing agent since it does not react with the alkylation reagent ABD-F, thus allowing reduction of disulfides and alkylation of the resulting sulfhydryls to be performed simultaneously. ABD-F is selective for cysteine and essentially nonfluorescent before reaction with sulfhydryls, providing a sensitive fluorescence assay for sulfhydryl groups (*28*, *29*). To a 0.1 mL aliquot of each HPLC fraction were added 0.95 mL of water and 0.15 mL of a freshly mixed solution of 1.0 M Na_3BO_3, pH 8.0, 8 mM EDTA, 2 mM TBP, and 0.1 mM ABD-F. The samples were incubated at 60 °C for 20 min, and then the relative fluorescence of each fraction was measured (excitation at 385 nm, emission at 520 nm). This reduction and fluorescent labeling allows identification of the tryptic HPLC fractions that contain cystine.

Identification of Disulfide-Containing NTPDase6 Tryptic Peptides. The remainder of the untreated HPLC tryptic fractions that showed increased ABD-F fluorescence were divided into two aliquots, one portion reduced with TCEP and the other portion not reduced. Reduction with TCEP was carried out by adjusting the pH of HPLC aliquots to 8.0−8.5 with ammonium hydroxide and adding TCEP to a final concentration of 0.2 mM (1 mM in some experiments), followed by incubation at 60 °C for 40 min. Both reduced and nonreduced aliquots were rechromatographed by HPLC, and the two peptide fractions from the reduced aliquot that eluted at different retention times than the nonreduced fraction (and therefore contain the two peptides involved in a disulfide bond) were collected. These fractions, as well as the original nonreduced fractions, were concentrated in a Speed Vac concentrator and submitted for MALDI-TOF mass spectral analysis. Peptides were identified by comparing peptide masses (*m*/*z*) obtained by MALDI-TOF MS with the theoretical masses of NTPDase6 tryptic peptides predicted by the PeptideMass program (http://us.expasy.org/cgi-bin/peptide-mass.pl).

Circular Dichroism. Spectra were acquired on an AVIV 215 circular dichroism spectrometer. Four scans from 300 to 180 nm of wild-type NTPDase6 at a protein concentration of 0.06 mg/mL in 10 mM Tris-HCl buffer were averaged and corrected for the small signal due to buffer. The data were converted into mean residue molar ellipticity, and the neural network K2D computer program (http://www.embl-heidelberg.de~andrade/k2d) was used to determine the percentage α-helix, β-sheet, and random coil based on the data collected from 200 to 240 nm (*30*). The PROF computer program was used to predict the secondary structural elements of NTPDase6 based solely on its primary structure (*31*).

RESULTS

Cloning, Expression, Refolding, and Purification of NTPDase6. We isolated a clone encoding NTPDase6 (CD39L2) from a human brain cDNA library, which is virtually identical in sequence to the CD39L2 protein reported earlier (*17*). After bacterial expression and purification of the resultant inclusion bodies, several parameters were evaluated for effects on the efficiency of refolding of active NTPDase6, including pH, ionic strength, and protein concentration. In addition, the presence/absence of detergents, divalent cations, concentration of redox reagents, and polar additives in the refolding buffer were all evaluated. An alkaline pH, the presence of L-arginine, and the redox pair of oxidized and reduced glutathione were each essential for the successful refolding of NTPDase6 from inclusion bodies into an active nucleotidase. Once an optimized refolding buffer was determined, the effect of temperature maintained during refolding was evaluated by refolding at several temperatures, ranging from 4 to 23 °C. For wild-type NTPDase6, optimum refolding occurred at 10−15 °C over 2−3 days.

Refolding time courses for both wild-type and C139S NTPDase6 were studied at 5, 13, and 23 °C (Figure 1), revealing the best refolding efficiency at 13 °C. Wild-type NTPDase6 showed decreasing activities at the extended time points, suggesting that the wild-type enzyme is not as stable as the C139S mutant under these conditions. This is especially evident at 23 °C, where the wild-type enzyme loses almost all activity after about 4 days at 23 °C. These results suggest that the mutant lacking the single free sulfhydryl is more stable than the wild-type NTPDase6 under these refolding conditions and that the removal of the single free sulfhydryl is beneficial for the folding of the protein.

The predicted molecular mass of the soluble, bacterially expressed 415-residue NTPDase6 pET28a construct after thrombin cleavage is 45.08 kDa. Figure 2 shows the SDS−PAGE analysis of both wild-type NTPDase6 (lane 2) and the C139S mutant (lane 3) after purification of the refolded proteins. The apparent molecular mass calculated from the standard protein calibration plot is 43 kDa, in good agreement with the theoretical mass after thrombin cleavage of the N-terminal hexahistidine tag. Western blotting of the bacterially expressed enzyme using an affinity-purified antibody

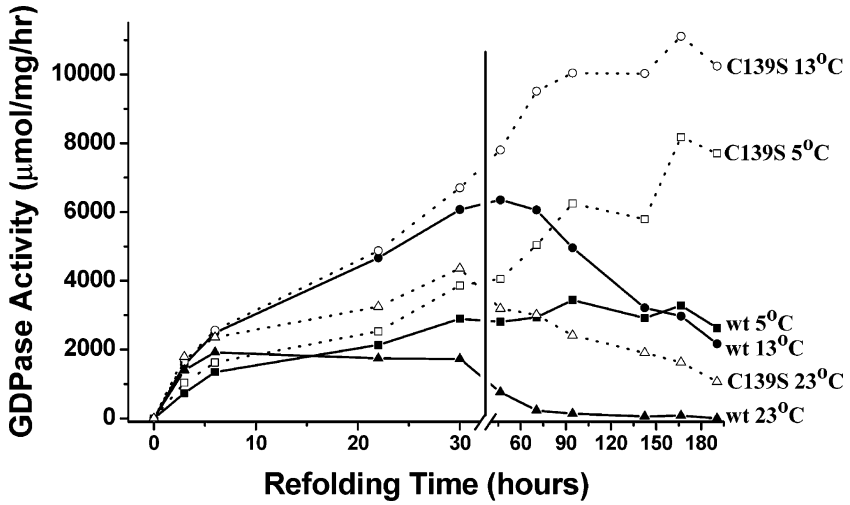

FIGURE 1: Refolding time course of wild-type and C139S NTPDase6 as a function of temperature. Inclusion body protein was denatured as described in Materials and Methods, refolded by dilution of 20 μL to a total volume of 1.0 mL, and incubated for the times and at the temperatures indicated in the figure. Wild-type NTPDase6 data are indicated by filled symbols, whereas C139S mutant data are represented by open symbols. In all samples, the refolding/dilution buffer contained 0.02 mg/mL protein in 150 mM Tris-HCl, 10 mM KCl, 250 mM NaCl, 2 mM $CaCl_2$, 2 mM $MgCl_2$, 800 mM L-arginine hydrochloride, 2 mM reduced glutathione (GSH), and 0.8 mM oxidized glutathione (GSSG), pH 8.3.

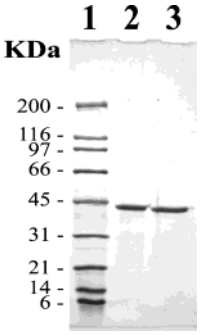

FIGURE 2: SDS−PAGE analysis of wild-type and C139S mutant NTPDase6 after refolding and purification. The samples were reduced and denatured prior to being loaded on a 4−15% gradient gel. Molecular mass standards are in lane 1. Lanes 2 and 3 show 2 μg of purified wild-type and C139S NTPDase6, respectively. After thrombin cleavage, NTPDase6 is a 415-residue protein, corresponding to a predicted molecular mass of 45.08 kDa.

raised against the C-terminal peptide sequence of NTPDase6 (*32*) showed an immunoreactive band at the same apparent molecular mass as seen in the Coomassie-stained gel shown in Figure 2 (data not shown).

Substrate Preference. As seen in Table 1, NTPDase6 expressed in bacteria preferentially hydrolyzes GDP, IDP, and UDP, with slower hydrolysis of CDP, ITP, GTP, CTP, ADP and UTP and virtually no hydrolysis of ATP. Previously published data on the mammalian cell (COS) expressed human soluble NTPDase6 showed a similar nucleotidase profile: GDP ≈ IDP > UDP > CDP > CTP > GTP > ITP > UTP > ADP > ATP (*19*). The substrate profile of bacterially expressed NTPDase6 is also consistent with results obtained using mammalian cell (CHO) expressed rat NTPDase6, reported by Zimmerman and co-workers to hydrolyze GDP > IDP ≫ UDP, CDP ≫ ADP (*18*). This rat homologue shares approximately 86% amino acid identity with human NTPDase6 (*18*, *19*).

The K_m of bacterially expressed wild-type NTPDase6 for GDP in the presence of Ca^{2+} was determined to be 130 ± 30 μM, while the K_m for the C139S mutant was 130 ± 40 μM. The same data gave fitted V_{max} values of 60000 ± 14000 and 48000 ± 8000 μmol mg^{-1} h^{-1} for the wild-type and C139S NTPDase6 enzymes, respectively. (All K_m and V_{max} values reported are the means ± standard deviations for five separate experiments.) Thus, both the wild-type and C139S bacterially expressed human NTPDase6 enzymes have K_m values for GDP similar to that of soluble rat NTPDase6 expressed in mammalian cells [211 ± 64 μM (*18*)].

Table 1: Substrate Preference of Wild-Type NTPDase6[a]

nucleotide substrate	nucleotidase activity (μmol mg^{-1} h^{-1})
ADP	1100 ± 50
ATP	110 ± 30
GDP	45000 ± 3700
GTP	2000 ± 500
IDP	25000 ± 3000
ITP	2700 ± 800
CDP	5800 ± 400
CTP	1700 ± 450
UDP	8900 ± 1200
UTP	560 ± 140

[a] The nucleotidase profile of NTPDase6 was generated by measuring activity in the presence of various nucleotide substrates, all at a final concentration of 2.5 mM, in the presence of 5 mM $CaCl_2$. A minimum of three experiments were performed (each in triplicate), and the nucleotidase activities are reported as the means ± standard errors (SE).

One previous study using mammalian cell expressed soluble NTPDase6 suggested that NTPDase6 GDPase activity is supported almost equally well by Ca^{2+} or Mg^{2+} (*18*), whereas another study indicated that NTPDase6 is considerably more active in the presence of Ca^{2+} than Mg^{2+} (*20*). To address this apparent discrepancy and to determine the pH dependence of activity (which has never been reported for NTPDase6), we assayed the GDPase activity of the refolded wild-type NTPDase6 over a pH range of 6.0−8.0 (Figure 3). As can be seen in Figure 3, the pH optimum for NTPDase6 GDPase activity is from 7.0 to 7.4, and the pH profiles for the enzyme activity in Ca^{2+} and Mg^{2+} are nearly identical, with the enzyme exhibiting slightly higher activity in Ca^{2+} versus Mg^{2+} buffer.

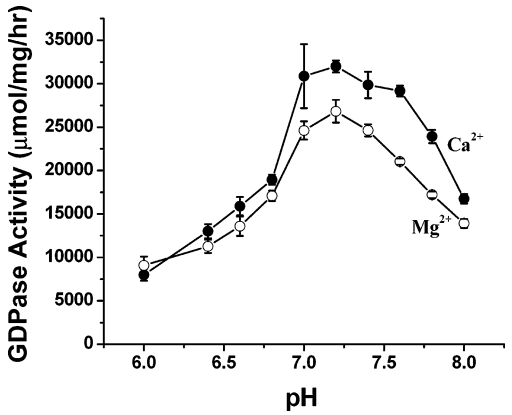

FIGURE 3: pH dependence of the hydrolysis of GDP by wild-type NTPDase6 in Ca^{2+} and Mg^{2+} MOPS buffers. GDP (2.5 mM) was used as the substrate for NTPDase6 in buffers containing 50 mM MOPS and either 5 mM Ca^{2+} (filled circles) or 5 mM Mg^{2+} (open circles) at the pH values indicated. The nucleotidase activity is reported as the mean of triplicate measurements ± standard error (SE).

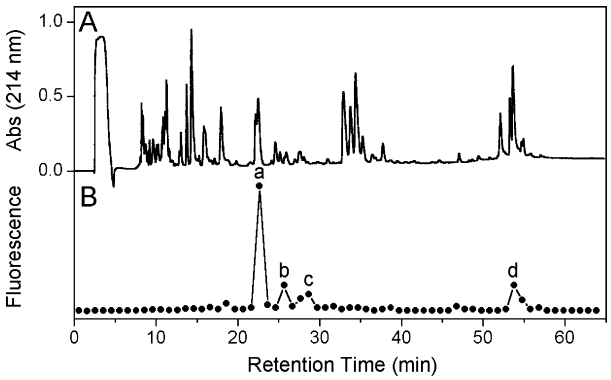

FIGURE 4: Peptide map of trypsin-digested NTPDase6. (A) Separation of NTPDase6 tryptic peptides by HPLC. Purified NTPDase6 (150 μg) was digested with trypsin and loaded onto a Vydac C_{18} column as described in Materials and Methods. Peptides were eluted with a gradient of acetonitrile in water containing 0.1% TFA. The solvent gradient profile went from 0% acetonitrile at 0 min to 10% at 6 min, to 20% at 14 min, to 32% at 44 min, and to 95% at 107 min, in linear segments. Only the portion of the gradient containing peptides is shown in the figure. One minute fractions were collected at a flow rate of 0.7 mL/min. (B) Fluorescence assay of HPLC fractions. Peptides in an aliquot from each fraction were reduced with TBP and alkylated with the sulfhydryl-specific reagent ABD-F, and the relative fluorescence of the resulting samples was measured using excitation at 385 nm and emission at 520 nm. The peaks labeled with a, b, c, and d indicate fractions with disulfide-containing peptides.

Determination of Cysteine Residues Involved in Disulfide Bonds. Figure 4A shows the peptide map of the tryptic digest of C139S NTPDase6. The fractions were assayed for the presence of disulfide bonds by measuring relative fluorescence after reduction and ABD-F labeling (Figure 4B). As is evident in Figure 4B, there are four labeled fractions containing disulfides (fractions eluting at 23, 26, 29, and 54 min and labeled a, b, c, and d, respectively, in the figure), rather than the two expected. This is most likely due to partial nonspecific cleavage of NTPDase6 protein at sites other than after Lys and Arg (see below). The remainder of the fractions containing the most fluorescent products were rechromatographed both with and without reduction, and the peptides with altered retention times after reduction (formerly disulfide-linked) were submitted for mass spectral analysis.

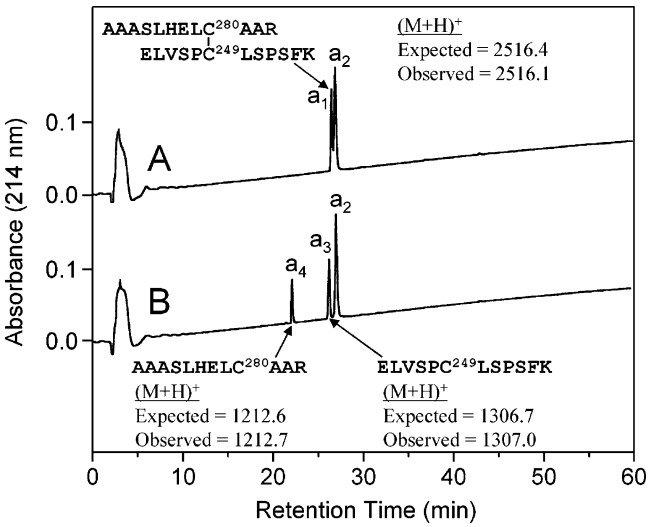

FIGURE 5: Separation and identification of peptides linked via Cys^{249}—Cys^{280}. Aliquots of fraction 23 (peak a in Figure 4B) were rechromatographed on the C_{18} column either without (A) or after (B) reduction by TCEP as described in Materials and Methods. Peptides were eluted with a gradient of acetonitrile in water containing 0.1% TFA. The HPLC solvent gradient profile used was from 0% acetonitrile at 0 min to 3% at 4 min, to 60% at 62 min, and to 95% at 65 min in linear segments. Only the portion of the gradient containing peptides is shown in the figure. One minute fractions were collected at a flow rate 0.7 mL/min. Peptides a_3 and a_4 in (B) are produced as a consequence of reduction of a disulfide-linked peptide present in peak a_1 in (A). Note that retention time of peak a_3 is slightly less than that of peak a_1, the latter disappearing after reduction. Reduction did not affect the retention time of peak a_2, indicating that peptides in this peak do not contain disulfides. Both nonreduced and reduced fractions were analyzed by MALDI-TOF MS. The monoisotopic masses and sequences of the identified peptides involved in a disulfide bond are shown in the figure.

This allowed identification of the peptides involved in the two disulfide bonds, Cys^{249}—Cys^{280} (Figure 5) and Cys^{340}—Cys^{354} (Figure 6). It should be noted that although the expected molar amounts of disulfides in fractions 23 and 54 (Figure 4B) are equal, the relative fluorescence of labeled peptides in fraction 23 (peak a in Figure 4B) is significantly higher than that in fraction 54 (peak d in Figure 4B). This is likely due to the large size and resultant high hydrophobicity of the peptide T^{342}—R^{371}, which is eluted as a disulfide-bonded peptide with the peptide Y^{338}—R^{341} in fraction 54. This peptide was reproducibly observed to bind strongly to the column and was recovered in poor yield upon rechromatography.

The peptide compositions of fractions 29 (peak c in Figure 4B) and 26 (peak b in Figure 4B), which also contain disulfides, were analyzed by MALDI-TOF MS. In these experiments, aliquots of fractions 29 and 26 were subjected to MALDI-TOF MS before and after reduction with TCEP, without rechromatography. In nonreduced fraction 29, peptides with masses $(M + H)^+$ of 2545.1 and 2559.7 were observed, which disappeared after reduction of the fraction. These peptides were identified as two disulfides. One disulfide was formed between peptide ELVSPC^{249}LSPSFK and peptide (G)QKAAASLHELC^{280}A(A) with expected mass 2545.3 and observed mass 2545.1 (here and below, amino acid residues neighboring the excised peptide are indicated in parentheses if cleavage occurred at sites other than after Lys or Arg). Another disulfide was formed

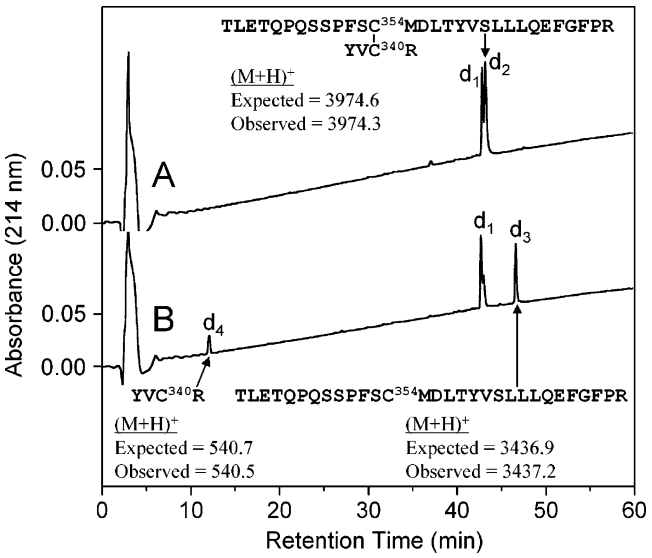

FIGURE 6: Separation and identification of peptides linked via Cys[340]−Cys[354]. Aliquots of fraction 54 (peak d in Figure 4B) were rechromatographed on a C_{18} column either without (A) or after (B) reduction by TCEP as described in Materials and Methods. The chromatographic conditions were the same as in Figure 5. Reduction of disulfides caused the decrease in the height of peak d_2 and appearance of peaks d_3 and d_4 in (B). The retention time of the heterogeneous peak d_1 was not affected by reduction, indicating that peptides in this peak do not contain disulfides. Analysis of nonreduced and reduced fractions by MALDI-TOF MS identified peptides involved in formation of a disulfide bond. The average masses and sequences of the peptides are shown in the figure.

between peptide ELVSPC[249]LSPSFK and peptide (A)ASLHELC[280]AARVS(E) with expected mass 2560.3 and observed mass 2559.7. In both of these disulfides, the same cysteine residues Cys[249]−Cys[280] are paired as in the main fraction 23 with the highest fluorescence (peak a in Figure 4B). Evidently, peptides in fraction 29 were formed due to tryptic cleavage of NTPDase6 at nonspecific protease sites.

In nonreduced fraction 26 (peak b in Figure 4B), a peptide with the monoisotopic mass $(M + H)^+$ of 2559.1 was observed, which disappeared after reduction. This peptide likely corresponds to a disulfide with expected mass of 2559.2, which is formed between peptide AAASLHELC[280]AAR and either peptide (Q)SSPFSC[354]MDLTYV(S) or peptide (S)SPFSC[354]MDLTYVS(L) (both latter peptides have the same mass and, therefore, cannot be differentiated by this mass spectral analysis). After reduction of fraction 26, peptides corresponding to AAASLHELC[280]AAR (expected mass 1212.6, observed mass 1212.5) and (Q)SSPFSC[354]MDLTYV(S) or (S)SPFSC[354]MDLTYVS(L) (expected mass 1349.6, observed mass 1349.5) were detected. Since in the major cystine-containing fraction 23 (peak a in Figure 4B), as well as in fraction 29 (peak c in Figure 4B), Cys[280] is disulfide-linked to Cys[249], the identification of a small amount of peptide containing a disulfide between Cys[280]−Cys[354] in fraction 26 (peak b in Figure 4B) suggests the presence of a small fraction of NTPDase6 molecules with mispaired cysteine residues. This minor fraction may derive from misfolded protein molecules that were not completely removed during purification. An alternative possibility is that this minor peptide containing the mispaired disulfide Cys[280]−Cys[354] was formed by disulfide interchange that occurred during trypsin proteolysis.

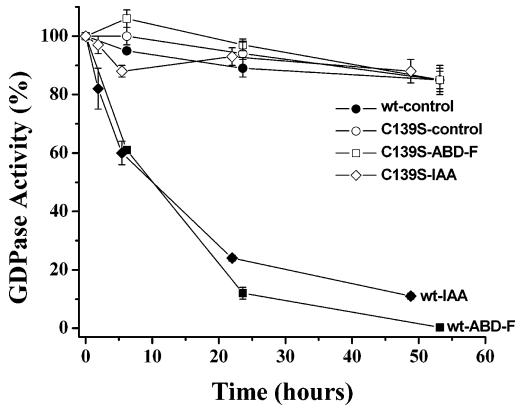

FIGURE 7: Inhibition of GDPase activity of wild-type NTPDase6 by iodoacetamide and ABD-F alkylation of Cys[139]. Wild-type (wt) and the C139S mutant of NTPDase6 (0.5−1.0 mg/mL) were incubated in buffer (20 mM Tris-HCl and 50 mM NaCl, pH 8.0) either without (controls) or with alkylation reagents [2 mM iodoacetamide (IAA) or ABD-F] at room temperature. Aliquots of enzymes were taken at the indicated time points and diluted with buffer (20 mM Tris-HCl and 50 mM NaCl, pH 8.0), and GDPase activities of the samples were assayed as described in Materials and Methods. Values represent the percentage of the activities of samples taken immediately after addition of alkylation reagents ("0" time point) and are given as means ± SD of three independent experiments.

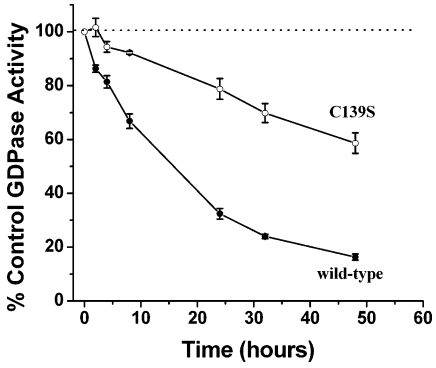

FIGURE 8: Inhibition of GDPase activity of wild-type NTPDase6 by H_2O_2 oxidation of Cys[139]. Wild-type (wt) and the C139S mutant of NTPDase6 (3.1−3.7 μg/mL) were incubated in buffer (20 mM Tris-HCl and 50 mM NaCl, pH 8.0) either without (for controls) or with 1 mM H_2O_2 at room temperature. Aliquots of enzymes were taken at the indicated time points, and GDPase activities of the samples were assayed as described in Materials and Methods. Values represent the percentage of the activities of control samples treated in parallel and are given as means ± SD of triplicate measurements.

Modification of the Single Free Sulfhydryl (Cys[139]) Residue in Wild-Type NTPDase6. Although the single unpaired cysteine (Cys[139]) is not essential for activity, since the C139S mutant has activity and properties very similar to that of the wild type, it was found that alkylation of this residue with either ABD-F or iodoacetamide resulted in loss of enzymatic activity (Figure 7). This suggests that although this residue is not directly involved in catalysis, it may be important for steric or, more likely, allosteric modulation of nucleotidase activity. Therefore, the effects of oxidation by 1 mM hydrogen peroxide at 22 °C of both wild-type and C139S NTPDase6 were investigated to determine if this single free sulfhydryl present in the wild-type enzyme (Cys[139]) was accessible to oxidation and if oxidation of this residue also inhibited activity. Figure 8 shows that the C139S mutant is less susceptible to oxidative inactivation than the wild-type

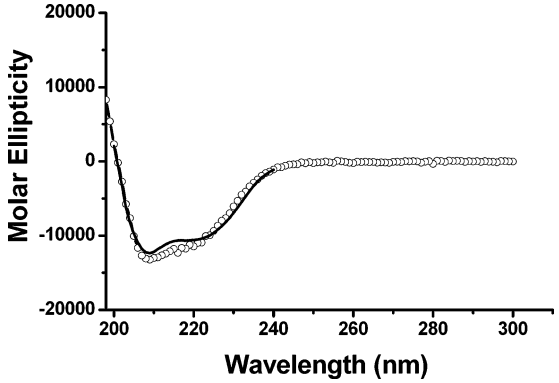

FIGURE 9: CD spectra of NTPDase6. The CD spectrum of wild-type NTPDase6 (open circles) is compared to the computer-predicted values derived from the primary structure (solid line). The CD spectra were acquired on an AVIV 215 spectrometer in 10 mM Tris-HCl buffer at a protein concentration of 1.3 μM. Four spectra were averaged and corrected for the small signal due to buffer absorption. The predicted CD spectrum was generated on the basis of the primary structure, using the PROF computer program, which is available on-line (see Materials and Methods).

NTPDase6 enzyme, indicating that oxidation of C139 is responsible for part of the inhibition of activity by oxidation of the wild-type NTPDase6 enzyme.

Circular Dichroism. The circular dichroism (CD) spectrum of wild-type NTPDase is shown in Figure 9. Deconvolution of the wild-type NTPDase6 CD spectra by conversion of the raw data (reported in millidegrees) to mean molar residue ellipticity and subsequent analysis by the K2D software program indicated that NTPDase6 was approximately 33% α-helix, 18% β-sheet, and 49% random coil. These results are consistent with the computed secondary structure (derived from primary structure analysis) using the PROF program (*31*), which predicts 31% α-helix, 20% β-sheet, and 49% random coil for NTPDase6.

Proposed Secondary Structure Model. A model incorporating the disulfide architecture, secondary structural elements predicted from the primary structure (and consistent with the analysis of the experimental CD spectrum of wt NTPDase6 shown in Figure 9), as well as data obtained from various analyses of other NTPDases, is shown in Figure 10. The model includes regions of amino acid conservation among the NTPDases termed *a*pyrase *c*onserved *r*egions [ACRs (*2*−*5*)] and phosphate binding sites [containing the consensus sequence DXG (*25*)] known to be involved in substrate interaction. Several proline residues conserved among the NTPDases are also indicated and are included in the model since they may serve as "breaks" in the secondary structural elements needed to properly position the apyrase conserved regions (ACRs) to allow favorable interactions with nucleotide substrates. The single unpaired cysteine residue (Cys^{139}) is located near one of the glycosylation sites (Asn^{144}), and chemical modification of that cysteine residue may inhibit enzyme activity allosterically, perhaps by changing the secondary and/or tertiary structure connecting ACR2 and ACR3. The two potential N-glycosylation sites, Asn^{144} and Asn^{208} (each containing the glycosylation consensus sequence NXT/S), are shown as glycosylated, since two previous studies showed that mammalian cell (COS) expressed soluble human NTPDase6 is glycosylated at both sites (*19*, *20*). However, it should be noted that bacteria are unable to perform many common posttranslational modifications including glycosylation, and therefore the NTPDase6 expressed in bacteria and studied in this work is not glycosylated. Nevertheless, the bacterially expressed, refolded, and purified NTPDase6 has a high specific activity, indicating that glycosylation is not essential for folding or nucleotidase activity of NTPDase6.

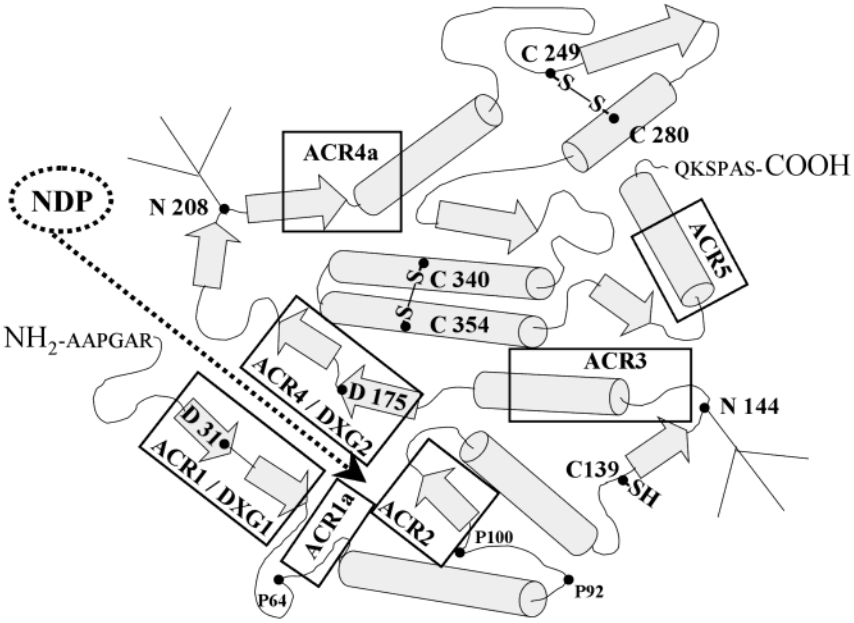

FIGURE 10: Secondary structure model of NTPDase6. This model incorporates the secondary structural elements as determined by CD and predicted from the primary structure, the disulfide architecture, regions of homology with other NTPDases termed apyrase conserved regions (ACRs), phosphate binding sites (DXG) known to be involved in substrate interaction, and conserved proline residues, which may be important for the proper spatial positioning of several of the secondary structural elements and ACRs. Seven extra amino acid residues that are derived from the expression vector and are present at the N-terminus of the bacterially expressed NTPDase6 are not shown. The numbering of amino acid residues starts from the N-terminal Ala shown in the figure, which is the beginning of the soluble NTPDase6 sequence after signal peptide cleavage (*19*).

DISCUSSION

The pET28a bacterial expression vector encodes both an N-terminal hexahistidine tag and a thrombin site to facilitate removal of the tag after purification of the expressed protein. The amino acid sequence of the NTPDase6 construct in pET28a is a 432 amino acid product, MGSSHHHHHHSS-GLVPR+GSHMASM**AAPG**...QKSPAS. The thrombin cleavage site is indicated by "+", and the start of the NTPDase6 soluble sequence (*19*) is underlined and indicated in bold face type. After thrombin cleavage, the 415 amino acid protein has seven "extra" amino acid residues at the N-terminus of the soluble NTPDase6, namely, GSHMASM. Thrombin cleaved and purified NTPDase6 migrates as a 43 kDa protein in SDS−PAGE (Figure 2), consistent with the predicted molecular mass of a monomer (45 kDa). Size exclusion gel analysis of the refolded and purified NTPDase6 is consistent with the active enzyme being a monomer (data not shown) and is in agreement with the results found for both the soluble human NTPDase6 expressed in COS cells (*19*) and the soluble NTPDase5 [CD39L4 (*33*)]. This is in contrast to the membrane-bound forms of the NTPDases, which all exist as homooligomers (*34*−*39*).

Refolding was accomplished by dilution of NTPDase6 into refolding buffers of varying compositions. Refolding by dialysis, which was efficient in our laboratory for refolding hSCAN-1 soluble human apyrase expressed in bacteria (*27*), was not successful for NTPDase6 using similar conditions. The effects of several additives known to increase protein stability and promote folding were examined in the refolding by dilution method. The efficiency of refolding was increased by the presence of the polar additive L-arginine (0.5−0.8 M) and by the redox pair of reduced and oxidized glutathione in the refolding buffer. Refolding was pH and temperature dependent, with the best refolding efficiency (indicated by nucleotidase activity) achieved at 10−15 °C at alkaline pHs. Given that the prevention of the mispairing of disulfide bonds should increase the efficiency of protein refolding, the sole nonconserved Cys^{139} residue in NTPDase6 was replaced by serine via site-directed mutagenesis. This mutation did improve the refolding properties of the enzyme, as is evident in Figure 1. The percentage of C139S NTPDase6 protein that refolded to the native state can be estimated from the purity of the inclusion body preparation (about 70% NTPDase6 protein), the activity of the crude protein after refolding (about 8000 μmol mg^{-1} h^{-1} using 2.5 mM GDP as substrate), and the activity of the pure protein (about 40000 μmol mg^{-1} h^{-1} using 2.5 mM GDP as substrate) to be approximately 28%. This efficiency is not as good as our laboratory obtained with the dialysis refolding of the hSCAN-1 soluble human nucleotidase [with an estimated efficiency of about 62% (*27*)] but is acceptable, considering that NTPDase6 contains two disulfide bonds and hSCAN-1 contains no disulfides which must be re-formed during refolding.

Replacement of the nonconserved Cys^{139} with serine did not substantially affect either the specific activity of the purified enzyme or the K_m for GDP hydrolysis. This indicates that Cys^{139} is not involved in the catalytic mechanism. However, either alkylation (Figure 7) or oxidation (Figure 8) of this residue decreased enzymatic activity, suggesting either a steric or an allosteric mechanism, possibly by perturbation of the secondary and/or tertiary structures connecting ACR2 and ACR3 (see Figure 10). The inhibition by oxidation is especially interesting in light of previously published studies indicating that other members of the NTPDase class of nucleotidases are inhibited by oxidation and that this process is physiologically relevant (*40*, *41*).

Zimmerman and co-workers reported that Ca^{2+} and Mg^{2+} stimulate the nucleotidase activity of rat NTPDase6 similarly, in agreement with our previous results obtained by expression of human NTPDase6 in COS cells (*19*). In contrast, Ford and co-workers reported that the nucleotidase activity of NTPDase6 expressed in COS cells was stimulated only 8-fold by Mg^{2+} compared to 17-fold by Ca^{2+}. Our results (Figure 3) indicate that bacterially expressed NTPDase6 can use either Ca^{2+} or Mg^{2+} nearly equally well to support its GDPase nucleotidase activity and that the maximal enzyme activity is achieved in the physiological pH range of 7.0−7.4.

Previous reports have demonstrated that NTPDase6 is expressed in mammalian cells as both a membrane-bound and a soluble glycoprotein, with 90% of the nucleotidase activity associated with the soluble form of the enzyme (*19*). Bacterially expressed, soluble human NTPDase6 reported in this work shows nucleotide substrate preference (Table 1) similar to the soluble, mammalian expressed human NTPDase6, characterized in an earlier publication (*19*), as well as to the soluble rat NTPDase6 expressed in CHO cells (*18*). Thus, soluble human NTPDase6 preferentially hydrolyzes nucleoside 5′-diphosphates over nucleoside 5′-triphosphates. ADP is the poorest nucleoside diphosphate substrate for this enzyme, consistent with these previous studies. In view of these results, the proposed functional role of NTPDase6 as a modulator of platelet aggregation by ADP hydrolysis seems doubtful, despite a relatively high level of expression of NTPDase6 in the heart (*20*).

The model shown in Figure 10 incorporates the findings in this work (e.g., the NTPDase6 disulfide bonds which are presumably conserved in all NTPDases) as well as previous findings obtained for NTPDase6 [e.g., the occupancy of the two putative glycosylation sites (*19*)] and general findings applicable to all NTPDases, including the existence of the apyrase conserved regions and several proline residues conserved in the NTPDases. The importance of a disulfide bond involving a conserved cysteine residue for the structure of the membrane-bound NTPDases was very recently demonstrated by mutation of Cys^{399} in NTPDase2 (also called ecto-ATPase or CD39L1). This mutation (Cys^{399} in NTPDase2 corresponds to Cys^{354} in NTPDase6 as revealed by multiple sequence alignments) led to production of an inactive and incorrectly processed NTPDase2 protein that was retained in the endoplasmic reticulum (*42*). Thus, the results presented in this study support those authors' interpretation that the perturbations observed after the mutation of Cys^{399} in NTPDase2 were due to the disruption of a disulfide bond, leading to an incorrectly folded and processed protein.

As also seen in Figure 10, the predicted secondary structural elements starting with both ACR1 and ACR4 are very similar to the actin superfamily protein secondary structure topology of $\beta\beta\beta\alpha\beta\alpha\beta\alpha$ starting with the phosphate binding domains (*43*). This is consistent with earlier results and hypotheses based on analysis of membrane-bound NTPDase3 and the importance of ACR1 and ACR4 for

enzyme activity (*25*). The two-dimensional model attempts to depict how many of the ACRs and structural features might come together in the three-dimensional structure of NTPDase6.

In summary, NTPDase6 (CD39L2) soluble human nucleotidase has been expressed in bacteria and refolded to a very high specific activity. The location of the two putatively conserved disulfide bonds has been determined, the lack of necessity of other posttranslational modifications for nucleotidase activity has been demonstrated, and a secondary structural model has been developed. Thus, the results presented in this study will assist attempts to determine the 3-D structure of this and other NTPDases. In addition, bacterial expression will facilitate site-directed mutagenesis experiments designed to elucidate the catalytic mechanism and determinants of substrate specificity, which could lead to the development of therapeutic proteins with modified nucleotide specificities (e.g., mutants having enhanced ADP hydrolysis could be useful as anticoagulants).

ACKNOWLEDGMENT

We thank Dr. Carrie Hicks-Berger for assistance with the characterization and sequencing of the human brain NTPDase6 clone used in this work, Drs. Evelyn Stimson and John Maggio for HPLC instrument time and assistance, Dr. James Ball for use of the fluorescence instrument, and Dr. Jack Howarth and Alex Dvoretsky for CD instrument time and assistance with CD measurements.

REFERENCES

1. Zimmermann, H., Beaudoin, A. R., Bollen, M., Goding, J. W., Guidotti, G., Kirley, T. L., Robson, S. C., and Sano, K. (1999) in *Second International Workshop on Ecto-ATPases and Related Ectonucleotidases* (Vanduffel, L., Ed.) pp 1−9, Shaker Publishing BV, Maastricht, The Netherlands, and Diepenbeek, Belgium.
2. Handa, M., and Guidotti, G. (1996) *Biochem. Biophys. Res. Commun. 218*, 916−923.
3. Kegel, B., Braun, N., Heine, P., Maliszewski, C. R., and Zimmermann, H. (1997) *Neuropharmacology 36*, 1189−1200.
4. Vasconcelos, E. G., Ferreira, S. T., De Carvalho, T. M. U., De Souza, W., Kettlun, A. M., Mancilla, M., Valenzuela, M. A., and Verjovski-Almeida, S. (1996) *J. Biol. Chem. 271*, 22139−22145.
5. Kirley, T. L., Yang, F., and Ivanenkov, V. V. (2001) *Arch. Biochem. Biophys. 395*, 94−102.
6. Marcus, A. J., Broekman, M. J., Drosopoulos, J. H. F., Islam, N., Alyonycheva, T. N., Safier, L. B., Hajjar, K. A., Posnett, D. N., Schoenborn, M. A., Schooley, K. A., Gayle, R. B., and Maliszewski, C. R. (1997) *J. Clin. Invest. 99*, 1351−1360.
7. Zimmermann, H. (1996) *Drug Dev. Res. 39*, 337−352.
8. Burnstock, G. (1996) *Lancet 347*, 1604−1605.
9. Chizh, B. A., and Illes, P. (2001) *Pharmacol. Rev. 53*, 553−568.
10. Marcus, A. J., Broekman, M. J., Drosopoulos, J. H., Pinsky, D. J., Islam, N., and Maliszewsk, C. R. (2001) *Ital. Heart J. 2*, 824−830.
11. Marcus, A. J., Safier, L. B., Hajjar, H. L., Ullman, H. L., Islam, N., Broekman, M. J., and Eiroa, A. M. (1991) *J. Clin. Invest. 88*, 1690−1696.
12. Pinsky, D. J., Broekman, M. J., Peschon, J. J., Stocking, K. L., Fujita, T., Ramasamy, R., Connolly, E. S., Jr., Huang, J., Kiss, S., Zhang, Y., Choudhri, T. F., McTaggart, R. A., Liao, H., Drosopoulos, J. H., Price, V. L., Marcus, A. J., and Maliszewski, C. R. (2002) *J. Clin. Invest. 109*, 1031−1040.
13. Gayle, R. B., Maliszewski, C. R., Gimpel, S. D., Schoenborn, M. A., Caspary, R. G., Richards, C., Brasel, K., Price, V., Drosopoulos, J. H. F., Islam, N., Alyonycheva, T. N., Broekman, M. J., and Marcus, A. J. (1998) *J. Clin. Invest. 101*, 1851−1859.
14. Kennedy, C., Todorov, L. D., Mihaylova-Todorova, S., and Sneddon, P. (1997) *Trends Pharmacol. Sci. 18*, 263−266.
15. Mihaylova-Todorova, S., Todorov, L. D., and Westfall, D. P. (2001) *J. Pharmacol. Exp. Ther. 296*, 64−70.
16. Todorov, L. D., Mihayalova-Todorova, S., Westfall, T. D., Sneddon, P., Kennedy, C., Bjur, R. A., and Westfall, D. P. (1997) *Nature 387*, 76−79.
17. Chadwick, B. P., and Frischauf, A. M. (1998) *Genomics 50*, 357−367.
18. Braun, N., Fengler, S., Ebeling, C., Servos, J., and Zimmermann, H. (2000) *Biochem. J. 351*, 639−647.
19. Hicks-Berger, C. A., Chadwick, B. P., Frischauf, A.-M., and Kirley, T. L. (2000) *J. Biol. Chem. 275*, 34041−34045.
20. Yeung, G., Mulero, J. J., McGowan, D. W., Bajwa, S. S., and Ford, J. E. (2000) *Biochemistry 39*, 12916−12923.
21. Kirley, T. L. (1997) *J. Biol. Chem. 272*, 1076−1081.
22. Stoscheck, C. M. (1990) *Anal. Biochem. 184*, 111−116.
23. Laemmli, U. K. (1970) *Nature (London) 227*, 680−685.
24. Fiske, C. H., and Subbarow, Y. (1925) *J. Biol. Chem. 66*, 375−400.
25. Smith, T. M., and Kirley, T. L. (1999) *Biochemistry 38*, 321−328.
26. Baykov, A. A., Evtushenko, O. A., and Avaeva, S. M. (1988) *Anal. Biochem. 171*, 266−270.
27. Murphy, D. M., Ivanenkov, V. V., and Kirley, T. L. (2003) *Biochemistry 42*, 2412−2421.
28. Kirley, T. L. (1989) *J. Biol. Chem. 264*, 7185−7192.
29. Kirley, T. L. (1989) *Anal. Biochem. 180*, 231−236.
30. Andrade, M. A., Chacon, P., Merelo, J. J., and Moran, F. (1993) *Protein Eng. 6*, 383−390.
31. Ouali, M., and King, R. D. (2000) *Protein Sci. 9*, 1162−1176.
32. Hicks-Berger, C. A., and Kirley, T. L. (2000) *IUBMB Life 50*, 43−50.
33. Mulero, J. J., Yeung, G., Nelken, S. T., Bright, J. M., McGowan, D. W., and Ford, J. E. (2000) *Biochemistry 39*, 12924−12928.
34. Stout, J. G., and Kirley, T. L. (1996) *Biochemistry 35*, 8289−8298.
35. Wang, T.-F., Ou, Y., and Guidotti, G. (1998) *J. Biol. Chem. 273*, 24814−24821.
36. Grinthal, A., and Guidotti, G. (2002) *Biochemistry 41*, 1947−1956.
37. Lewis Carl, S. A., Smith, T. M., and Kirley, T. L. (1998) *Biochem. Mol. Biol. Int. 44*, 463−470.
38. Murphy, D. M., Ivanenkov, V. V., and Kirley, T. L. (2002) *J. Biol. Chem. 277*, 6162−6169.
39. Caldwell, C. C., Hornyak, S. C., Pendleton, E., Campbell, D., and Knowles, A. F. (2001) *Arch. Biochem. Biophys. 387*, 107−116.
40. Robson, S. C., Kaczmarek, E., Siegel, J. B., Candinas, D., Koziak, K., Millan, M., Hancock, W. W., and Bach, F. H. (1997) *J. Exp. Med. 185*, 153−163.
41. Krotz, F., Sohn, H. Y., Keller, M., Gloe, T., Bolz, S. S., Becker, B. F., and Pohl, U. (2002) *Arterioscler. Thromb. Vasc. Biol. 22*, 2003−2009.
42. Mateo, J., Kreda, S., Henry, C. E., Harden, T. K., and Boyer, J. L. (2003) *J. Biol. Chem.* (in press).
43. Hurley, J. H. (1996) *Annu. Rev. Biophys. Biomol. Struct. 25*, 137−162.

BI035137R